Statistical study of the quasi-perpendicular shock ramp widths

Y Hobara, M Balikhin, V Krasnoselskikh, M Gedalin, H Yamagishi

▶ To cite this version:

Y Hobara, M Balikhin, V Krasnoselskikh, M Gedalin, H Yamagishi. Statistical study of the quasi-perpendicular shock ramp widths. Journal of Geophysical Research Space Physics, 2010, 115, A11106 (8 p.). 10.1029/2010JA015659 . insu-01180745

Statistical study of the quasi-perpendicular shock ramp widths

Y. Hobara,[1,2] M. Balikhin,[2] V. Krasnoselskikh,[3] M. Gedalin,[4] and H. Yamagishi[5]

Received 11 May 2010; revised 12 July 2010; accepted 13 August 2010; published 18 November 2010.

[1] The width of the collisionless shock front is one of the key shock parameters. The width of the main shock transition layer is related to the nature of the collisionless process that balances nonlinearity and therefore leads to the formation of the shock itself. The shock width determines how the incoming plasma particles interact with the macroscopic fields within the front and, therefore, the processes that result in the energy redistribution at the front. Cluster and Themis measurements at the quasi-perpendicular part of the terrestrial bow shock are used to study the spatial scale of the magnetic ramp. It is shown that statistically the ramp spatial scale decreases with the increase of the shock Mach number. This decrease of the shock scale together with previously observed whistler packets in the foot of supercritical quasi-perpendicular shock indicates that it is the dispersion that determines the size of magnetic ramp even for supercritical shocks.

Citation: Hobara, Y., M. Balikhin, V. Krasnoselskikh, M. Gedalin, and H. Yamagishi (2010), Statistical study of the quasi-perpendicular shock ramp widths, *J. Geophys. Res.*, *115*, A11106, doi:10.1029/2010JA015659.

1. Introduction

[2] Collisionless shocks (CS) are ubiquitous in space, they play an important role in the solar wind interaction with the planets, they also are believed to have vital importance for such a fundamental astrophysical problem as cosmic ray acceleration. CS are of crucial importance for understanding physical processes in the vicinity of such astrophysical objects as supernova remnants, plasma jets, binary systems and ordinary stars. From this great variety of CS in the Universe only those in the solar system can be a subject of in situ observations. Moreover, comprehensive in situ data exist only for interplanetary shocks and planetary bow shocks. It is worth noting that some astrophysical shocks are similar to those in the solar system. The main process that takes place at the collisionless shock is the redistribution of the energy of the directed bulk plasma motion to the plasma thermalization and acceleration of small part of plasma particles to high energies. The physical processes that determine the energy redistribution and particle acceleration processes are crucially dependent upon the characteristic scales in the transition region of the shock. In addition, spatial scales are closely related to the shock structure and formation, because they are determined by the processes that counterbalance steepening of the shock front due to the nonlinearity.

[3] In the case of the ordinary gas dynamics the redistribution of the directed flow energy occurs at the shock front due to the particle collisions. It is these collisions that stop steepening of the shock, which results in the formation of the front on the spatial scales of the order of the mean free path. In the case of collisionless plasma, anomalous processes of plasma interaction with fields and waves in the shock replace particle collisions and lead to the energy redistribution. This is most evident for subcritical shocks. Subcritical shocks are weak shocks for which anomalous resistivity alone can provide enough dissipation to satisfy Rankine-Hugoniot conditions that required for a formation of a stationary shock [*Kennel et al.*, 1985]. The nonlinear process of steepening of a nonlinear structure can be described as the energy transfer to smaller scales. The steepening can be terminated either by collisionless dissipation of wave dispersion. If the dissipative scale L_d exceeds the dispersive one L_{disp}, the former is reached first and further steepening is ceased by the dissipation that takes away energywhich would otherwise cascaded to even smaller scales. When steepening is balanced by dissipation, a dissipative subcritical shock forms. Such a shock is characterized by a monotonic transition in the magnetic field (magnetic ramp) of the width $\sim L_d$. The dissipative length is determined by some anomalous process like generation of intense waves and their dissipation. However, most subcritical collisionless shocks observed in situ are dispersive. The dispersive shock is formed when $L_{disp} > L_d$. In this case further steepening is prevented by the short-scaledispersive waves which are able to propagate away from the forming front. These waves effectively remove the energy which would be otherwise transferred to even smaller scales. In perpendicular shocks (where the normal to the shock front is almost perpendicular the upstream magnetic field) the phase velocity of the dispersive waves decreases with the decrease of the scale and a wave trail is formed downstream of the magnetic ramp. In oblique geometry the phase velocity increases with the decrease of the spatial scale and an upstream wave train is formed. The upstream wave pre-

[1] Department of Electronic Engineering and Research Station on Seismo Electromagnetics, University of Electro-Communications, Chofu, Japan.
[2] ACSE, University of Sheffield, Sheffield, UK.
[3] LPCE, CNRS, Orleans, France.
[4] Department of Physics, Ben-Gurion University, Beer-Sheva, Israel.
[5] National Institute of Polar Research, Tokyo, Japan.

0148-0227/10/2010JA015659

cursor is phase standing in the upstream flow. Its amplitude decreases with the distance from the shock ramp due to dissipation processes as it was discussed in early theoretical papers describing subcritical shocks [*Sagdeev*, 1965]. Dispersive shocks were at first described by *Sagdeev* [1965] [see also *Biskamp*, 1973]. The structure of the dispersive shock front is determined by the balance between the dispersion and nonlinearity. If the upstream velocity becomes too high, the small amplitude waves that form the most distant (from the shock wave) packets are no longer able to phase stand in the plasma flow, and, therefore, can no longer form a stationary precursor. The question whether the front of a high Mach number supercritical shock (the terrestrial bow shock and most of other planetary bow shocks belong to this group) is in the dispersive regime or not is still open. One of the strongest indications in favor of the dispersive regime are the whistler wave packets often observed upstream of quasi-perpendicular shocks.

[4] The conventional classification distinguishes between subcritical and supercritical shocks. Subcritical shocks are assumed to be formed when the anomalous resistivity (sometimes together with assistance of anomalous viscous processes [*Kennel et al.*, 1985]) can provide sufficient dissipation of the bulk flow kinetic energy. It is possible only if the Mach number does not exceed the so-called first critical Mach number M_{c1}. If the Mach number is high enough, the energy dissipation is due to the reflection of a fraction of upstream ions [*Leroy et al.*, 1982].

[5] It is believed that the transition to the supercritical reflection shock occurs when the downstream bulk flow velocity exceeds the downstream thermal velocity of ions. Supercritical reflection shocks have a more complex structure in comparison to subcritical shocks. If the angle between the shock normal and the upstream magnetic field $\theta_{Bn} > 45°$, the shock is called quasi-perpendicular. In such a shock a reflected ion making excursion upstream of the flow gains additional energy from the tangential component of the electric field, and after that crosses the shock front. Hereafter we are interested in quasi-perpendicular shocks only. The turnaround of the reflected ions in this case occurs because the upstream magnetic field does not allow most of the reflected ions to travel far upstream turning them back to the shock front. The upstream region, where the beam of the reflected ions performs part of their Larmor orbit before being turned back to the shock, is called a foot. The foot is characterized by the 15%–20% increase in the magnitude of the magnetic field. The analysis of a Larmor orbit of a specularly reflected ion gives a good estimate of the spatial size of the foot as $L_f = 0.68R_{Li} \sin \theta_{Bn}$, where R_{Li} is the upstream ion convective gyroradius [*Woods*, 1969; *Livesey et al.*, 1984]. Taking into account the nonspecular character of the ion reflection, the above estimate is somewhat modified toward smaller values [*Gedalin*, 1996]. Downstream of the main transition of the quasi-perpendicular shock the gyration of the bulk plasma ions together with the gyration of the beam of reflected ions leads to an overshoot-undershoot structure. The size of the overshoot and undershoot can be estimated straightforwardly in terms of the ion gyroradius. However, the major transition layer, where the plasma parameters change most rapidly (namely, the sharpest increase of the magnetic field magnitude and plasma density and the sharpest decrease of the flow velocity occur), lies between the foot and the overshoot and is the thinnest part of the shock front. This layer in a supercritical quasi-perpendicular shock is traditionally characterized by the steepest increase of the magnetic field referred to as the ramp. The major jump in the electrostatic potential, the ion reflection, and the electron thermalization occur within the ramp. Although the ion thermalization will take place at much larger distances downstream of the ramp, it is the ramp spatial scale that is supposed to determine the characteristics of the major physical processes which are responsible for the formation of the shock front structure, and the mechanisms of the shock front interaction with the incoming flows of electrons and ions. For instance, the potential electric field can develop a small-scale substructure inside the ramp, which is expected to occur within the front of high Mach number shocks and leads to the front nonstationarity [*Krasnoselskikh*, 1985; *Galeev et al.*, 1988a, 1988b; *Krasnoselskikh et al.*, 2002]. Such decrease of the characteristic scale should lead to the electron demagnetization and efficient nonadiabatic heating of electrons [*Balikhin et al.*, 1993; *Balikhin and Gedalin*, 1994].

[6] When the ramp scale in the shock front is determined by the dispersion-nonlinearity interplay, another critical Mach number, M_w, becomes important, which is associated with the precursor wave train that is formed upstream of the quasi-perpendicular shock. The parameter M_w is determined by the maximum velocity of small amplitude whistler waves. When the Mach number M exceeds this whistler critical M_w the standing stationary precursor wave train cannot be formed anymore. As we already mentioned the precursor role is the evacuation of the excess of energy to prevent further steepening. If a stationary precursor is impossible it can be expected that the shock becomes nonstationary [*Krasnoselskikh et al.*, 2002]. However, in the case of such nonstationarity the typical spatial scale of the magnetic ramp is still determined by the nonlinear whistler spatial scale and the characteristic ramp width l_r would be proportional either to $c\cos\theta_{Bn}/\omega_{pi}$ or to c/ω_{pe} [*Galeev et al.*, 1988a, 1988b; *Gedalin*, 1998; *Krasnoselskikh et al.*, 2002].

[7] Single satellite missions provide very poor possibilities for reliable identification of the shock widths and characteristic scale evaluation of the fine structure of the shock front. The spatial size of the foot or overshoot have been used for comparative estimates [*Balikhin et al.*, 1995]. On the contrary, multisatellite missions such as Cluster and THEMIS provide good new opportunities for a comprehensive study of the shock ramp scales. Cluster data have been used already for statistical studies of the shock front thickness of supercritical quasi-perpendicular shocks [*Bale et al.*, 2003]. In that paper a hyperbolic tangent function have been fitted to the shock transition layer. The authors concluded that the spatial scale of the quasi-perpendicular shock transition is of the order of the convective gyroradius of the upstream ions. Fitting a hyperbolic or exponential function leads to mixing spatial scales of the foot and the ramp. Since the ramp is much thinner, the resulting scale will correspond to the scale of the foot rather than that of the ramp. The present paper is devoted to statistical studies of the magnetic field spatial scales in the ramp region of the

shock front using Cluster and THEMIS observations. Four closely spaced Cluster spacecraft allow more reliable separation of spatial and temporal variations. However, the Cluster orbit allows one to study mainly the shocks away from the ecliptical plane with Mach numbers that are in the lower range of the whole space of Mach numbers, since the shock normal deviates from the sunward direction. To increase the range of available Mach numbers, THEMIS shock crossings were added to the Cluster set. Magnetic ramps cannot be always treated as uniform. Nonlinear substructures have been observed and reported within the ramp in several cases [e.g., *Balikhin et al.*, 2002; *Walker et al.*, 2004]. The study of spatial-temporal characteristics of such substructures requires at least two point measurements separated by a distance that is sufficiently smaller then inter satellite distances in both THEMIS and Cluster missions, thus we leave the substructure analysis beyond the scope of the present paper, and restrict ourselves with the study of the ramp spatial scales only.

2. Data Sets

[8] It is possible to estimate the spacecraft velocity with respect to bow shock on the basis of single-spacecraft measurements, using the duration of the crossing of the foot region, provided the spatial size of this region is known. However, only the data from multisatellite missions allow one to unambiguous separate between spatial and temporal variations, and only the use of multipoint data sets can provide reliable determination of shock scales. In the present study the data from both current multisatellite missions, Cluster and THEMIS, are used for a statistical study of the spatial size of the ramp of the terrestrial bow shock. Both these missions gained comprehensive data on the terrestrial bow shock and assembled a huge stockpile of shock crossings. It is worth noting that they complement each other because of the difference in their orbits. The THEMIS orbit is close to equatorial plane providing an opportunity to sample the terrestrial bow shock in the vicinity of the subsolar point. Cluster crossings of the terrestrial bow shock occur mainly on the flanks. The solar wind flow in the vicinity of the terrestrial orbit is almost along Sun-Earth line, so that the Mach numbers of flank shocks are relatively low due to the greater deviation of the local shock normal from the sunward direction. Therefore, the combination of THEMIS and Cluster crossings leads to a greater dynamical range of Mach numbers available for the analysis than each of these missions provides separately. Cluster crossings for two time intervals, February–April 2001 and February–March 2002, have been investigated in the present study. Theses time intervals have been chosen based on the availability of Cluster archive data at the beginning of this study orbit geometry suitable for clear observations of quasi-perpendicular part of terrestrial bow shock. THEMIS shock crossings included in the present study took place from the beginning of July 2007 to the end of August 2007. The magnetic field data used in the present paper came from Cluster and THEMIS fluxgate magnetometers (FGM) [*Balogh et al.*, 1997; *Auster et al.*, 2008]. The data from the initial phase of the THEMIS mission are also used in the present study to ensure that THEMIS C and D spacecraft separation is not very large.

3. Criteria for Choosing Shocks and Definition of Notions "Size" and "Scale" Used in Our Study

[9] The study of the spatial scale of the shock ramp requires transformation from temporal to spatial variables. The crucial issue for such a study is an accurate estimate of the relative shock spacecraft velocity along the shock front normal. To solve this problem it is required to perform reliable identification of the local normal to the shock front. To calculate the model shock normal we used the model shape of the terrestrial bow shock identified by *Farris et al.* [1991]. These values of the shock normal were then compared with those found making use of the methods based on timing differences between the 4 Cluster spacecraft shock crossings, minimum variance and coplanarity theorem, and finally were validated using the evolution of the magnetic field component along the normal direction B_n. The only shock selection criteria that we applied to sets of Cluster and THEMIS shocks crossings, that were registered during the time period under consideration, was related to reliability of the shock normal identification. Those shock crossings, for which the calculated normal could not be considered reliable (because of the B_n evolution or due to large discrepancy in the shock normal directions found by different methods), have been excluded from this study. The relative shock spacecraft velocity V_{ss} has been calculated using the shock normal direction, satellite separation vectors and time delay between two subsequent shock crossings. The ramp crossing duration was defined as a time interval between the upstream edge of the ramp and the maximum of overshoot. The spatial size (width) of the magnetic ramp has been estimated as a product of V_{ss} and the duration Δt of the ramp crossing. In addition to the spatial width of the magnetic ramp the concept of the ramp spatial scale (gradient scale) has been used.

[10] The main motivation for the study of the magnetic ramp width L_r is that it is this scale that determines the nature of the shock, i.e., the dominant physical processes that counteract nonlinear steepening. According to the ideas proposed by *Galeev et al.* [1988a, 1988b] the characteristic scale of the shock front is nothing but the scale of the nonlinear whistler solitary structure. If it is the case the width will be determined as the thickness of the solitary structure which is standing in the reference frame of the Earth, and moving with the solar wind velocity toward upstream in the reference frame of solar wind plasma. Another possibility might be the characteristic anomalous resistivity dissipation scale length determined by some instability, either of low hybrid waves as have been proposed by *Papadopoulos* [1985], or ion acoustic waves as was suggested by *Galeev* [1976], or modified Buneman instability considered by *Matsukio and Scholer* [2006]. In other words, the determination of this scale can allow one to answer the question whether the ramp structure is determined by dispersive or dissipative effects, and provide an indication what kind of the process dominates.

[11] Another important parameter that characterizes the ramp transition is the characteristic gradient scale. The motivation for introducing this ramp gradient spatial scale is

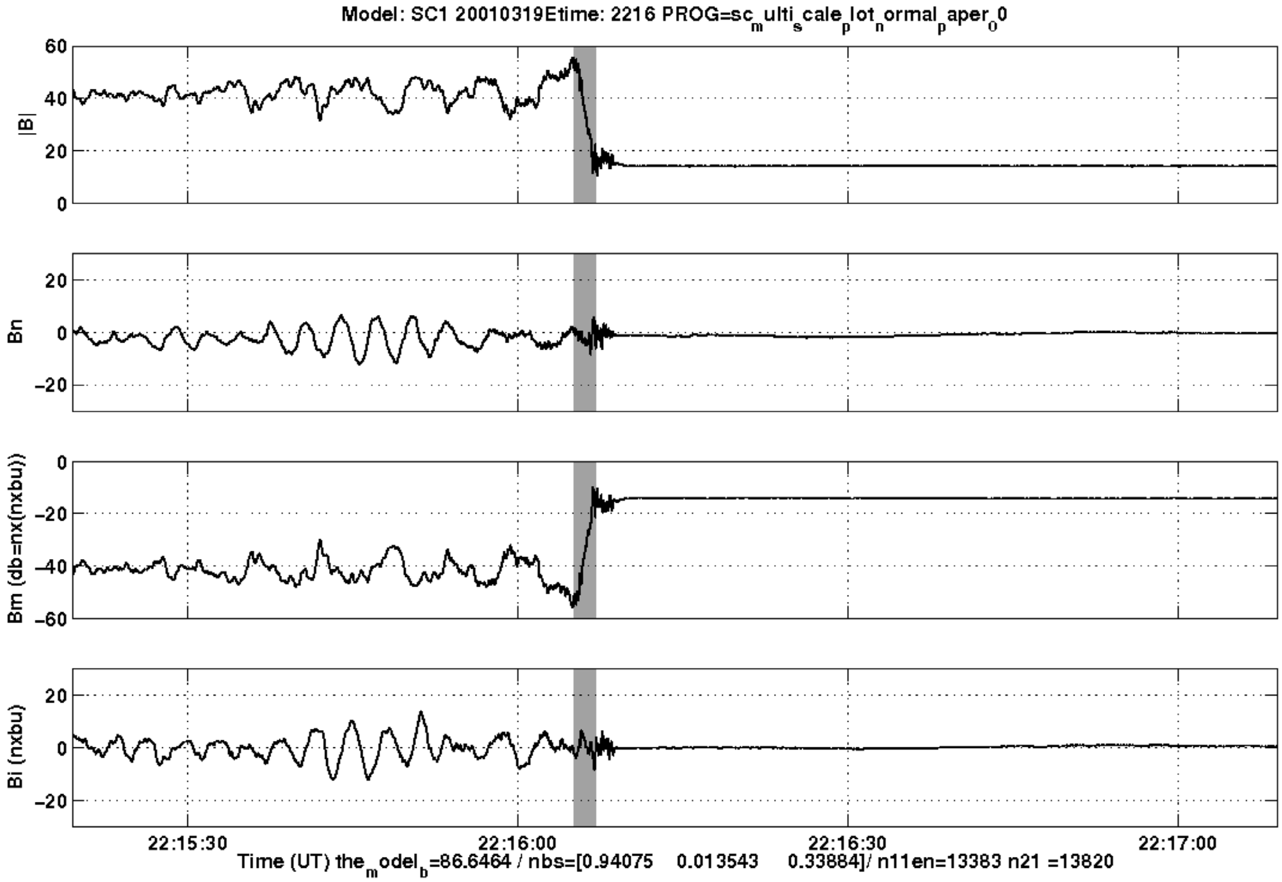

Figure 1. The magnitude and three components of the magnetic field as measured by Cluster 1 magnetometer on 19.03.2001 during the crossing of the terrestrial bow shock.

related to two major physical processes that are very important for shock physics. First is the interaction of incoming electrons with the electromagnetic field at the shock front. As it was shown by *Balikhin et al.* [1993], *Balikhin and Gedalin* [1994], *Gedalin et al.* [1995a, 1995b], and *Balikhin et al.* [1998], an important effect of violation of the adiabaticity in such interaction can occur even if the width of the magnetic ramp considerably exceeds the formally calculated electron gyroradius. The parameter that determines the transition from adiabatic to nonadiabatic electron dynamics is the characteristic gradient of the electromagnetic fields. This effect can be understood taking into account the ability of the inhomogeneous electric field within the ramp to demagnetize electrons by straightening their paths which results in the increase of the effective gyroradius. The parameter that determines the demagnetization is the magnetic field characteristic gradient normalized to the background magnetic field, namely $\frac{1}{l_d} = \frac{\nabla|B|}{B_0}$. Another important effect is related to the stability of the ramp region of the shock. According to *Krasnoselskikh* [1985] and *Galeev et al.* [1988a, 1988b] the nonlinear whistler wave structure becomes unstable when the characteristic gradient overcomes some critical value. When this happens the dispersion can no longer balance the nonlinearity and the shock front overturns [*Krasnoselskikh*, 1985]. The characteristic gradient scale represents a rather universal characteristic of the steepness of the shock front, which is the main reason for statistical study of the magnetic ramp spatial gradient scale in addition to the ramp width (size).

[12] The set of shocks that have been used for the study of statistical properties of the ramp width and gradient scale in the present paper includes 77 crossings of the terrestrial bow shock (30 by THEMIS and 47 by Cluster). As it was mentioned above the main criterion for a shock to be included in this set is the reliability of the identification of the shock normal. To illustrate the analysis we perform, in Figure 1 we present one of the typical shock profiles from the data set used. Three components of the magnetic field B_n,B_m,B_l, together with the field magnitude $|B|$, as measured by Cluster 1 spacecraft during the crossing of the terrestrial bow shock on 19.03.2001 at 22:16:10 UT are plotted in Figure 1. B_n is the component parallel to the identified shock normal n. Another components are chosen as follows. Unit vector e_m is in the plane of the upstream magnetic field and perpendicular to the shock normal. The e_l direction completes the system and corresponds to the noncoplanar component of the magnetic field within the ramp. B_n component undergoes rather low level of fluctuations at the time when ramp crossing is evident from $|B|$. The level of fluctuations is less then 10% of the magnetic field change within the ramp. This indicates that the direction n has been determined with the accuracy sufficient for the aims of the present study. The shock front has a well defined foot, ramp and overshoot regions with the ratio of downstream to

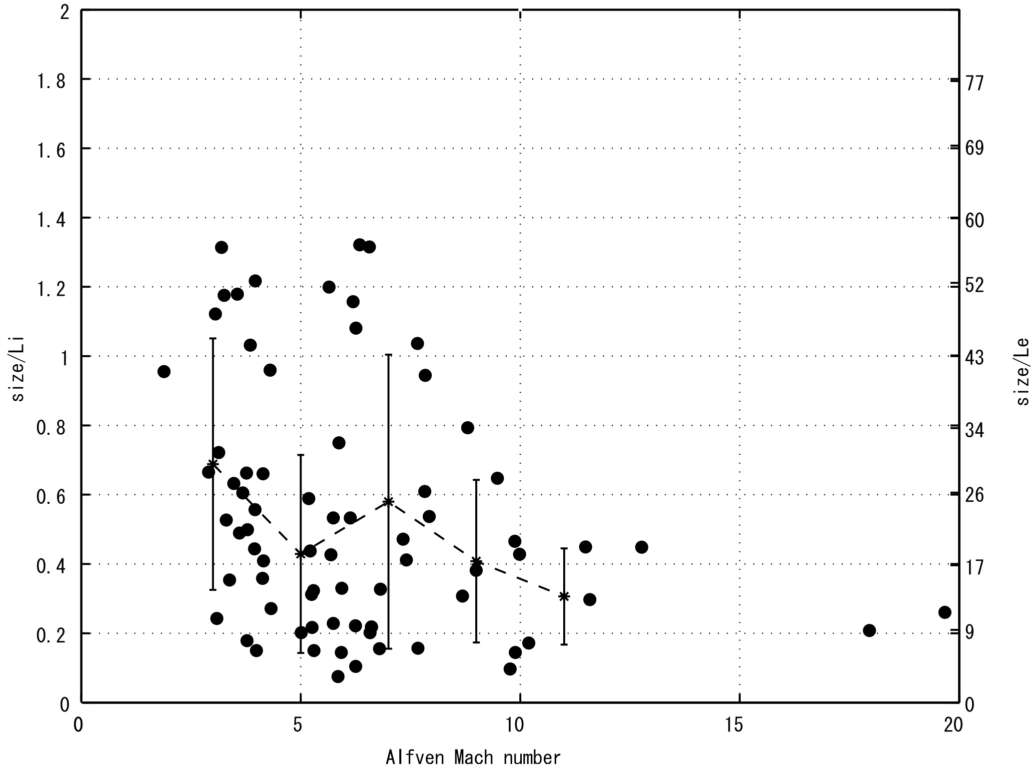

Figure 2. Scatterplot of experimentally derived shock size normalized on the ion inertial scale length $\frac{c}{\omega_{pi}}$ (left axis) and electron inertial scale $\frac{c}{\omega_{pe}}$ (right axis) as a function of Alfven Mach number. The dashed line represents the averaged values of shock width averaged over shocks with Alfven Mach number in the ranges 2–4, 4–6, 6–8, 8–10, 10–12. The vertical lines represent the statistical error bars for each range of Mach numbers 2–4, 4–6, 6–8, 8–10, and 10–12.

upstream magnetic field at about 2.2 indicating that it is not especially strong quasi-perpendicular shock. Indeed, calculated Alfvenic Mach number, and the angle between the shock normal and the upstream magnetic field are about M = 4.1 and θ_{Bn} = 85° correspondingly. The estimated ramp width for this particular shock is about $L_r = 0.66L_i$ while the spatial scale corresponding to the steepest increase of the magnetic field in the ramp about $L_d = 0.26L_i$, where $L_i = \frac{c}{\omega_{pi}}$ is the ion inertial length.

[13] The scatterplot of the ramp spatial sizes as a function of Alfven Mach number is shown in Figure 2. The width of the magnetic ramp varies by about an order of magnitude from as wide as about $L_r = 1.4L_i$ ($\approx 60L_e$) to $0.1L_i$ ($\approx 4L_e$). The general trend in Figure 2 indicates that the magnetic ramp becomes thinner with the increase of Alfvenic Mach number. This trend is evident even without taking into account two shock crossings with peculiarly high Mach numbers M in the range 17–20 that correspond to two markers in the bottom right corner of the scatterplot. Another tendency that should be noted is the decrease of the maximum of the shock front width with the increase of the Mach number. To make these tendencies more clear we present here also the characteristic width of the magnetic ramp averaged for the shocks with Alfvenic Mach numbers in ranges 2–4, 4–6, 6–8, 8–10 and 10–12 (dashed curve). The vertical lines on Figure 2 represent the statistical error bars for each range of Mach numbers 2–4, 4–6, 6–8, 8–10 and 10–12. The decrease of statistical errors with the Mach number is in complete accordance with the significant decrease of the maximum shock width, while the minimum shock width undergoes much smaller changes.

[14] Figure 3 shows the scatterplot of the spatial gradient scale of the magnetic ramp. It clearly demonstrates the same features that were evidenced in Figure 2 for the ramp width: a quite wide range of values, especially for low Mach number shocks and the trend toward shorter scales with the increase of the Mach number as well as the decrease of the maximum gradient scale while Mach number increases. As the change of the magnetic field for all chosen shocks exceeds B_0 (for many of them quite significantly) the values of the gradient scale are smaller then the width of the corresponding shocks. The ramp gradient spatial scale varies in the range 0.05–0.82L_i (2–35L_e).

4. Discussion and Conclusions

[15] As we have already noted above the main goal of the present investigation of the ramp spatial scales is to establish the major physical process that can balance nonlinearity, terminate steepening and form the major transition of the shock front, ramp. Theoretical studies of the dynamics and formation of the dispersive shock front [*Galeev et al.*, 1988a, 1988b; *Gedalin*, 1998; *Krasnoselskikh et al.*, 2002] predict that the spatial gradient scale of the ramp should decrease with the Mach number. As it was first shown for low Mach number shocks the phase standing whistler wave

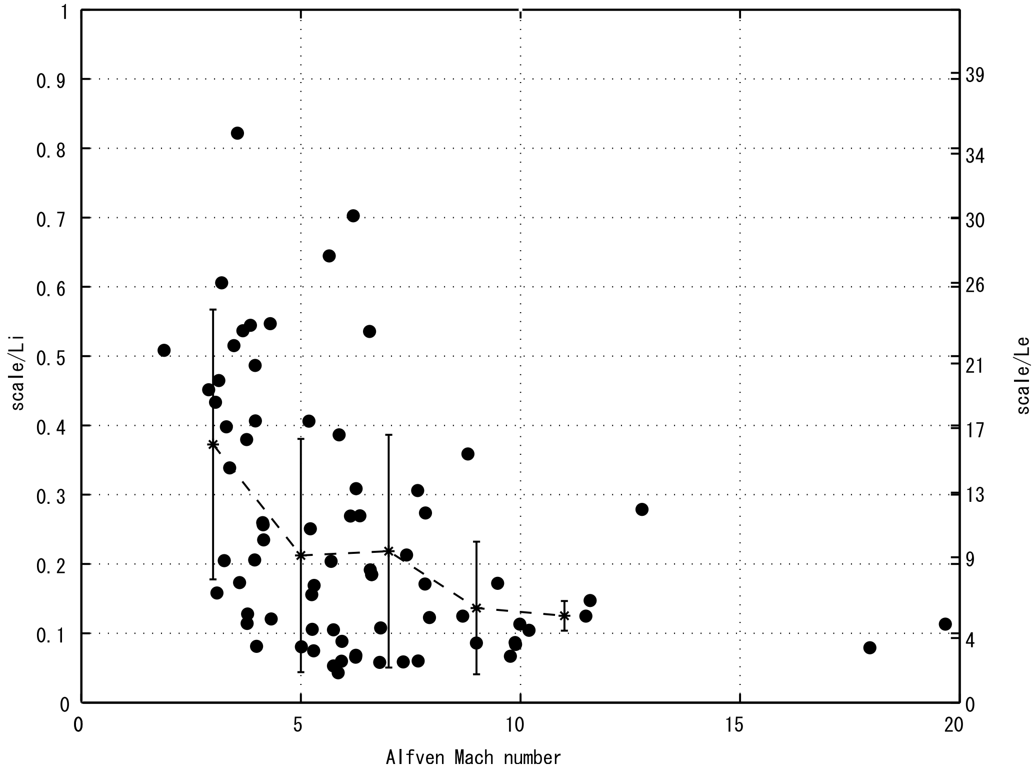

Figure 3. Scatterplot of experimentally derived shock spatial scale normalized on the ion $\frac{c}{\omega_{pi}}$ (left axis) and electron $\frac{c}{\omega_{pe}}$ (right axis) inertial lengths as a function of Alfven Mach number. The dashed line represents the values of the shock spatial scale averaged over shocks with Alfven Mach number in the ranges 2–4, 4–6, 6–8, 8–10, 10–12. The vertical lines represent the statistical error bars for each range of Mach numbers 2–4, 4–6, 6–8, 8–10, and 10–12.

forms the transition layer of the shock front that implies the condition that the phase velocity of such a wave $\frac{\omega}{k}$ should be equal to the upstream bulk velocity of the solar wind flow $M_a\ v_a$. The dispersion relation for the whistler waves,

$$\omega = \Omega_e \cos\theta_{Bn} \frac{k^2 c^2}{\omega_{pe}^2}$$

means increase of the phase and group velocities of linear and nonlinear waves with the k vector, i.e., inversely proportional to the characteristic scale

$$V_{ph} \sim V_{gr} \sim k \sim \frac{1}{l}.$$

Taking into account that the phase and group velocities are proportional to the Alfvenic Mach number one can infer

$$l \sim \frac{1}{M_A}.$$

This dependence still holds for nonlinear whistler waves in high Mach number flows even if the small amplitude part of wave precursor is not able to be established as phase standing in the incoming flow. The effect of the flow deceleration can complicate this dependence, however the major tendency that the characteristic gradient scale decreases with the increase of Mach number remains valid. Our statistical analysis unambiguously confirms this dependence.

[16] It must be noted that the statistical study of spatial scales associated with electric field structures observed within the supercritical shock transition layer *Walker et al.* [2004], indicated similar dependence upon Mach number as found in the present paper for the ramp scale. However, *Walker et al.* [2004]shows that the sizes associated with the electric field structures are on average considerably smaller than the magnetic ramp size. Most of the structures studied by *Walker et al.* [2004] are shorter than 10 $\frac{c}{\omega_{pe}}$ and only very few exceed 20 $\frac{c}{\omega_{pe}}$.

[17] This is not surprising as many structures studied by *Walker et al.* [2004] have been observed within the magnetic ramp.

[18] An alternative model proposed by *Hada et al.* [2003] describes the formation of the monotonous profile of the electrostatic potential that has spatial scale larger than the magnetic field transition. In this model the dependence of the scale of the ramp is similar to the scale dependence of the foot formed by reflected ions, i.e,. gradient scale would be proportional to Mach number which is at odds with our observations. Another class of models came from the numerical simulations of *Matsukio and Scholer* [2006]. These simulations show the growth of instabilities due to the relative motion of different groups of particles (modified two stream instability, modified Buneman instability). The development of the instabilities results in the deceleration of the flow and formation of a wide transition layer where the

ramp does not differ much from the preceding oscillations. In this case there is no clearly pronounced dependence upon the scale, it is determined by the instability conditions. Our observations do not confirm such effects.

[19] It is worth noting that the results of simulations are strongly dependent upon the mass ratio of electrons and ions (in the simulations by *Matsukio and Scholer* [2006] the ratio is realistic, in contrast with the simulations by *Lembege and Savoini* [1992] and upon the ratio of plasma to gyro frequencies ($\frac{\omega_{pe}}{\Omega_e}$). The last one for the case of the Earth bow shock is about 100–200 while in the above mentioned simulations it is about 2–4. This ratio determines the refractive index of whistler waves, and its underestimate results in a very large overestimate of the electric to magnetic field ratio. This strongly affects the wave particle interaction and can easily explain the appearance of such artifacts of simulations as the ion accumulation in the vicinity of the shock front due to the artificial overestimate of the potential and electromagnetic electric fields.

[20] To summarize, the results of our statistical study clearly show the decrease of the ramp gradient characteristic scale with the Mach number and therefore strongly support the models describing the ramp as an evolving nonlinear whistler wave [*Galeev et al.*, 1988a, 1988b; *Gedalin*, 1998; *Krasnoselskikh et al.*, 2002]. Our results do not confirm the results of *Bale et al.* [2003] and this contradiction is related to the methodology used in the latter paper. Fitting hyperbolic tangent function to the shock transition layer led to the mixing of two shock front regions with drastically different physics, the foot and the ramp. It was well known before *Bale et al.* [2003] that such mixing should lead to the absorption of the shorter ramp scale by much more wide foot.

[21] The present statistical study leads to another important conclusion concerning the possibility of electron nonadiabatic heating in front of the terrestrial bow shock, caused by strong inhomogeneity of electric and magnetic fields in the ramp [*Balikhin et al.*, 1993, 1995, 1998]. In Figure 2 one can see that there are several very thin shocks with the characteristic width less then $4L_e$ similar to the one observed by *Newbury and Russell* [1996]. It also can be seen from Figure 3 that for a 20% of shocks the ramp spatial scale is $4L_e$ or even shorter. As typical β for upstream plasma is of the order of one, one can conclude that the deviations from the adiabatic motion of electrons and as a result overadiabatic heating should be observed for a substantial number of shocks.

[22] **Acknowledgments.** Authors are grateful to the Royal Society for support of a collaboration project between UK and Japan. The work of Sheffield group on this paper has been supported by STFC. The work of V.K. was supported by CNES grant “Cluster Co-I DWP.” V.K., M. G., and M.B. are grateful to ISSI for financial support of this work in the framework of the team activities entitled “High Mach number collisionless shock dynamics: Theory and simulations versus multipoint measurements in space.” M.G. was partially supported by ISF grant 275/07.

[23] Philippa Browning thanks Heng Qiang Feng and another reviewer for their assistance in evaluating this paper.

References

Auster, H. U., et al. (2008), The THEMIS fluxgate magnetometer, *Space Sci. Rev.*, *141*, 235.

Bale, S. D., F. S. Mozer, and T. S. Horbury (2003), Density-transition scale at quasi-perpendicular collisionless shocks, *Phys. Rev. Lett.*, *91*, 265004, doi:10.1103/PhysRevLett.91.265004.

Balikhin, M. A., and M. A. Gedalin (1994), Kinematic mechanism of electron heating in shocks: Theory vs observations, *Geophys. Res. Lett.*, *21*, 841.

Balikhin, M. A., M. E. Gedalin, and A. Petrukovich (1993), New mechanism for electron heating in shocks, *Phys. Rev. Lett.*, *70*, 1259.

Balikhin, M. A., M. E. Gedalin, and V. Krasnoselskikh (1995), The scales in quasiperpendicular shocks, *Adv. Space Res.*, *15*, 247.

Balikhin, M. A., V. Krasnoselskikh, L. J. C. Woolliscroft, and M. A. Gedalin (1998), A study of the dispersion of the electron distribution in the presence of E and B gradients: Application to electron heating at quasi-perpendicular shocks, *J.Geophys. Res.*, *103*, 2029.

Balikhin, M. A., et al. (2002), Observation of the terrestrial bow shock in quasi-electrostatic subshock regime, *J. Geophys. Res.*, *107*(A8), 1155, doi:10.1029/2001JA000327.

Balogh, A., et al. (1997), The cluster magnetic field investigation, *Space Sci. Rev.*, *79*, 65.

Biskamp, D. (1973), Collisionless shock waves in plasmas, *Nucl. Fusion*, *13*, 719.

Farris, M. H., S. M. Petrinec, and C. T. Russell (1991), The thickness of the magnetosheath: Constraints on the polytropic index, *Geophys. Res. Lett.*, *18*, 1821.

Galeev, A. A. (1976), Collisionless shocks, in *Physics of Solar Planetary Environment*, edited by D. J. Williams, pp. 464, AGU, Washington, D. C.

Galeev, A. A., V. Krasnoselskikh, and V. Lobzin (1988a), Fine structure of the front of a quasiperpendicular supercritical collisionless wave, *Sov. J. Plasma Phys.*, *14*, 697.

Galeev, A. A., C. F. Kennel, V. Krasnoselskikh, and V. Lobzin (1988b), The role of whistler oscillations in the formation of the structure of high Mach number collisionless shock, in *Proceedings of the Joint Varenna-Abastumani International School and Workshop on Plasma Astrophysics Held in Varenna, Italy*, edited by T. D. Guyenne, *ESA Spec. Publ.*, *285*, 165.

Gedalin, M. (1996), Ion reflection at the shock front revisited, *J. Geophys. Res.*, *101*, 4871.

Gedalin, M. (1998), Low-frequency nonlinear stationary waves and fast shocks: Hydrodynamical description, *Phys. Plasmas*, *5*, 127.

Gedalin, M. A., K. A. Gedalin, M. A. Balikhin, and V. V. Krasnoselskikh (1995a), Demagnetization of electrons in the electro-magnetic field structure, typical for quasi–perpendicular shock, *J. Geophys. Res.*, *100*, 9481.

Gedalin, M. A., K. A. Gedalin, M. A. Balikhin, V. V. Krasnoselskikh, and L. J. C. Woolliscroft (1995b), Demagnetization of electrons in inhomogeneous $E \perp B$: Implications for electron heating in shocks, *J. Geophys. Res.*, *100*, 19,911.

Hada, T., M. Oonishi, B. Lembege, and P. Savoini (2003), Shock front nonstationarity of supercritical parpendicular shock, *J. Geophys. Res.*, *108*(A6), 1233, doi:10.1029/2002JA009339.

Kennel, C. F., J. P. Edmiston, and T. Hada (1985), A quarter century of collisionless shock research, in *Collisionless Shocks in the Heliosphere: A Tutorial Review*, *Geophys. Monogr. Ser.*, vol. 34, edited by R. G. Stone and B. T. Tsurutani, pp. 1, AGU, Washington, D. C.

Krasnoselskikh, V. (1985), Nonlinear motions of a plasma across a magnetic field, *Sov. Phys. JETP, Engl. Transl. 62*(2), 282–288.

Krasnoselskikh, V., B. Lembege, P. Savoini, and V. Lobzin (2002), Nonstationarity of strong collisionless quasiperpendicular shocks: Theory and full particle numerical simulations, *Phys. Plasmas*, *9*, 1192.

Lembege, B., and P. Savoini (1992), Nonstationarity of a two dimensional quasiperpendicular supercritical collisionless shock by self-reformation, *Phys. Fluids*, *4*, 11.

Leroy, M. M., D. Winske, C. C. Goodrich, C.S. Wu, and K. Papadopoulos (1982), The structure of perpendicular bow shocks, 87, *J. Geophys. Res.*, 5081.

Livsey, W. A., C. T. Russell, and C. F. Kennel (1984), A comparison of specularly reflected gyrating ion orbits with observed shock foot thicknesses, *J. Geophys. Res.*, *89*, 6824.

Matsukio, S., and M. Scholer (2006), On microinstabilities in the foot of high Mach number perpendicular shocks, *J. Geophys. Res.*, *111*, A06104, doi:10.1029/2005JA011409.

Newbury, J. A., and C. T. Russell (1996), Observations of a very thin collisionless shock, *Geophys. Res. Lett.*, *23*, 781.

Papadopoulos, K. (1985), Microinstabilities and anomalous transport, in *Collisionless Shocks in the Heliosphere: A Tutorial Review*, *Geophys. Monogr. Ser.*, vol. 34, edited by R. G. Stone and B. T. Tsurutani, pp. 59, AGU, Washington, D. C.

Sagdeev, R. Z. (1965), Collisionless shocks, in *Reviews of Plasma Physics*, edited by M. A. Leontovich, translated from Russian, vol. 4, pp. 23, Consult. Bur., New York.

Walker, S. N., H. Alleyne, M. A. Balikhin, M. Andre, and T. Horbury (2004), Electric field scales at quasi-perpendicular shocks, *Ann. Geophys. 22*, 2291.

Woods, L. C. (1969), On the structure of collisionless magneto-plasma shock waves at supercritical Alfven- Mach numbers, *J. Plasma Phys.*, *3*, 435.

M. Balikhin and Y. Hobara, ACSE, University of Sheffield, Sheffield S10 2TN, UK.

M. Gedalin, Department of Physics, Ben-Gurion University, PO Box 653, Beer-Sheva 84105, Israel.

V. Krasnoselskikh, LPCE, CNRS, 3A, Ave. de la Recherche Scientifique, F-45071 Orleans CEDEX 2, France.

H. Yamagishi, National Institute of Polar Research, 10-3, Midoricho, Tachikawa, Tokyo 190-8518, Japan.